Quantum field theory of atoms interacting with photons. II. Scattering of short laser pulses from trapped bosonic atoms

L. You,[1] Maciej Lewenstein,[1,2] and J. Cooper[3]
[1] *Institute for Theoretical Atomic and Molecular Physics, Harvard-Smithsonian Center for Astrophysics, 60 Garden Street, MS 14, Cambridge, Massachusetts 02138*
[2] *Centrum Fizyki Teoretycznej, Polska Akademia Nauk, 02-668 Warsaw, Poland*
[3] *JILA, University of Colorado and National Institute of Standards and Technology, Boulder, Colorado 80309-0440*
(Received 13 December 1994)

We discuss a method for probing a system of cold bosonic atoms in a trap using intense short laser pulses. Above the critical temperature for Bose-Einstein condensation, such a system scatters very weakly. Coherent scattering occurs primarily in the forward direction within a solid angle determined by phase matching conditions for the thermal atomic distribution. Below the critical temperature, the number of scattered photons increases dramatically and the scattered light is emitted into a solid angle determined by the size of the condensate. Quantum statistics of the atoms explicitly effect the spectrum as well as the squeezing properties of the scattered light. The theory accounts for the atom-atom interactions.

PACS number(s): 03.75.Fi, 42.50.Fx, 32.80.−t

I. INTRODUCTION

The experimental realization of a Bose-Einstein condensate (BEC) [1] in a system of trapped and cooled atoms [2] has recently become one of the major objectives of atomic physics [3]. Significant progress has been achieved in the last year toward this goal. Three groups [4] have now reported the observation of evaporative cooling [5] in laser precooled alkali-metal-atom systems. New techniques have been developed to cool spin polarized hydrogen [6]. In this context it becomes urgent to consider in detail problems concerning the detection and observation of the condensate.

One of the most obvious methods for observing the condensate consists of light scattering, as is used in standard spectroscopic studies. Until now, most of the theoretical studies on the quantum optics of BEC consider the problem of weak field scattering. Svistunov and Shlyapnikov [7] and Politzer [8] discuss the problem of scattering of weak light from the condensate at low temperatures $T \simeq 0$. In a homogeneous system, the atomic and photonic degrees of freedom mix, giving rise to a band gap in the excitation spectrum. Of course, in practice the gap appears only in the narrow line limit, i.e., when the gap width significantly exceeds the spontaneous emission rate γ. Because of this gap, resonant light will be strongly reflected back from the sharp boundary of the condensate. Javanainen considered another limiting case, that of an optically thin condensate [9], with a size a of the order of the resonant wavelength λ. In such a case the scattering takes place mainly in the forward direction, and the scattering cross section has a Lorentzian line shape with a width proportional to the collective (superradiant) spontaneous emission width (which typically would be of the order of $\gamma n\lambda^2 a$, where n is the atomic density). Note, that these conclusions are significantly modified in more realistic situations, i.e., in an optically thick trap with no sharp boundaries and of finite size a ranging from 1 to 20 λ. In the case of moderate atomic densities n such that $n(\lambda/2\pi)^3 \simeq$ 1–10, the elastic weak field spectrum becomes non-Lorentzian and exhibits a narrow peak at the resonance. The width of this narrow feature is controlled by the dominant single-atom dissipative and dephasing processes such as spontaneous emission to noncondensed states, quantum diffusion of the excited atomic wave packets [10], etc.

In a recent Letter [11] we proposed yet another method for optical detection of BEC. We investigated the limiting case of the scattering of short but intense laser pulses from a system of cooled atoms in a trap. In particular, we considered laser pulses with areas of multiples of 2π. The area of the pulse is defined as the integral of the slowly varying envelope of the electric field multiplied by the atomic dipole moment. When the area is $2\pi K$, the atom cycles K times between the excited and ground state. We have shown that above the critical temperature for the Bose-Einstein condensation, T_c, the coherent scattering from such a system of atoms is very weak and takes place primarily in the forward direction due to the phase matching effects. Below the critical temperature the number of scattered photons increases dramatically and the coherent scattering occurs into a solid angle determined by the size of the condensate. Even below T_c, sufficiently short $2\pi K$ pulses leave the system relatively intact, providing a nondemolition tool for observing BEC.

In a previous paper (hereafter called paper I) [12] we formulated a general framework for the quantum field theoretical description of atoms interacting with photons. We discussed various approximations, including the case of scattering of short but intense laser pulses off cold atomic samples. We introduced several classes of models of the theory and discussed regimes of their applicability: (i) class A models that neglect all static atom-atom interactions; (ii) class B models that account fully for excited-ground atom-atom interactions; and finally (iii) class C models that take into account all relevant atom-atom interactions.

This paper, which is the second in the series, contains a detailed discussion of the problem of scattering of intense short laser pulses. As outlined in paper I, we focus our attention on the range of parameters describing magnetic traps such as those developed by Monroe *et al.* [13]. For simplicity we consider the strong field scattering for two-level atoms with a ground s state and a triple degenerate excited p state. The same assumption was adapted in Ref. [11].

We start our discussion by considering the class A models that neglect all static atom-atom interactions. In Sec. II we present a detailed derivation of the results presented in Ref. [11]. The calculations are performed in the Fock representation of the quantized atomic fields. Section III is devoted to the calculation of coherent and incoherent spectra emitted in the process of scattering of intense short laser pulses. In Sec. VI we discuss numerical results for the spectra of scattered light for typical values of parameters that are of interest to experiments. These results provide an extension of the results reported in Ref. [11]. In Sec. V we calculate the squeezing spectra of the scattered field, and show that in homodyne type measurements, the scattered field might exhibit broad-band super-Poissonian statistics, with a narrow band of sub-Poissonian and squeezing behavior at the exact resonance.

We reformulate our theory in Sec. VI using the position representation for the atomic fields. With this reformulation it is particularly simple to extend the theory to class B and class C models where atom-atom interactions are included. The effects of atom-atom interactions can be shown to be negligible within the duration of the driving laser pulse. Their main effect (that effects the long time behavior of the system) is to set appropriate initial conditions for the system prior to the interaction with the laser pulse. Within this framework we can calculate scattering spectra for class B or C models, and compare them with the results obtained for noninteracting atoms. Finally, we conclude in Sec. VII.

The paper also contains four appendixes. In Appendix A, we list some useful identities characterizing atomic states in a harmonic trap. Appendixes B, C, and D contain details of the calculations of various parts of the spectra of scattered light.

II. CLASS A MODELS IN THE FOCK REPRESENTATION

The Hamiltonian governing the interaction of light with N bosonic atoms confined in a trap takes the following second quantized form in the Fock representation [12]:

$$\begin{aligned}\mathcal{H} &= \sum_{\vec n}\omega^g_{\vec n} g^\dagger_{\vec n} g_{\vec n} + \sum_{\vec m}(\omega^e_{\vec m}+\omega_0)\vec e^{\,\dagger}_{\vec m}\vec e_{\vec m} \\ &\quad + \sum_{\vec n,\vec m}\sum_{\mu}\int d\vec k\,\varrho(k)\left[\eta_{\vec n\vec m}(\vec k) g^\dagger_{\vec n} a^\dagger_{\vec k\mu}\vec e_{\vec m}\cdot\vec \epsilon_{\vec k\mu} + \text{H.c.}\right] \\ &\quad + \sum_{\mu}\int d\vec k\; ck\; a^\dagger_{\vec k\mu} a_{\vec k\mu}. \qquad (1)\end{aligned}$$

In Eq. (1) we have used the rotating wave approximation, as well as the dipole approximation in the length gauge. The Hamiltonian is written in atomic units. The symbols $g_{\vec n}$ ($g^\dagger_{\vec n}$) denote atomic annihilation (creation) operators for the $\vec n$th state of the center of mass motion of the atom in the trap. These operators are associated with the atoms in the ground electronic state. For a rotationally invariant harmonic trap potential, $\vec n$ is actually a triple index (n_x, n_y, n_z), and the corresponding energy is $\omega^g_{\vec n} = \omega_t(n_x+n_y+n_z)$, where ω_t is the trap frequency. The size of the trap in this work is related to the size of the ground state of the trap potential, $a=\sqrt{1/2M\omega_t}$ (for notation and some useful identities, see Appendix A). The latter relation can be relaxed for so called class A^* models that account phenomenologically for the effects of (repulsive) atom-atom interactions. One then treats a and ω_t as independent parameters and sets $a>\sqrt{1/2M\omega_t}$ [12,10] to mimic an interacting condensate. The operators $\vec e_{\vec m}$ ($\vec e^{\,\dagger}_{\vec m}$) are atomic annihilation (creation) operators in the excited state trap potential, which, in general, is different from the ground state potential. The results of our analysis of short pulse scattering do not depend strongly on the particular shape of the excited state potential. The corresponding energies are $\omega_{\vec m}+\omega_0$, i.e., they are shifted up by the electronic transition frequency. We consider here the case of the transition from an s state to a p state and therefore $\vec e_{\vec m}$'s and $\vec e^{\,\dagger}_{\vec m}$'s have a corresponding vector character. This is not the structure of the transition in a typical alkali-metal atom such as cesium ($6S_{1/2}$, F = 4–$6P_{3/2}$, F = 5), but the character of the transition is not essential for our conclusions. $a_{\vec k\mu}$ and $a^\dagger_{\vec k\mu}$ denote annihilation and creation operators for photons of momentum $\vec k$ and linear polarization $\vec\epsilon_{\vec k\mu}$ ($\mu=1,2$). All the annihilation and creation operators obey standard bosonic commutation relations. The coupling $\varrho(k)$ is a slowly varying function of k related to the natural linewidth (half width at half maximum) $\gamma=(8\pi^2k_0^2/3c)\left|\varrho(k_0)\right|^2$, with $k_0=\omega_0/c$. Finally, $\eta_{\vec n\vec m}(\vec k)$ are the Franck-Condon factors (i.e., matrix elements for the center of mass transition from the $\vec n$th state of the ground state potential to the $\vec m$th state of the excited state potential),

$$\eta_{\vec n\vec m}(\vec k) = \langle g,\vec n|e^{-i\vec k\cdot\vec R}|e,\vec m\rangle. \qquad (2)$$

To keep the notation simple, we will omit the indices g, e for the internal states in the following. We will use the convention that the indices $\vec n$, $\vec n'$ ($\vec m$, $\vec m'$) denote the center of mass states in the electronic ground (excited) state potentials, respectively.

The above Hamiltonian includes the strong resonant atomic dipole-dipole interaction resulting from the exchange of transverse photons [14,15]. In this section, we treat class A models, and neglect all other interactions that may play a crucial role in atomic collisions.

If the system is driven by a short coherent laser pulse, and if such a pulse is strong enough and short enough, we may neglect spontaneous emission effects during the pulse and substitute the electric field operator entering the interaction Hamiltonian in Eq. (1) by a c number. The pulses we intend to use should have duration $\tau_L \leq$ 300 ps or shorter, i.e., width $\gamma_L = 1/\tau_L \simeq (3\times10^9)-10^{11}$ Hz. The first estimate shows that indeed $\gamma_L \gg \gamma \simeq 2.5$ MHz, i.e., the spontaneous emission may be legitimately neglected during the time of interaction of the pulse with the atoms. Note, however, that this estimate is misleading, since the atoms will respond collectively and the effective spontaneous emission rate (due to both superradiant initial state enhancement and bosonic final state enhancement) might thus be greatly enhanced [16]. We will therefore have to check our assumption self-consistently to assure that the total number of emitted photons $N_{\rm tot}$ is much smaller than the total number of atoms N. Unfortunately, the substitution of the electric field operator by a c-number field during the interaction also eliminates from the theory the effects of resonant dipole-dipole interactions. The self-consistency check related to $N_{\rm tot}$ is not necessarily sufficient to assure that the effects related to level shifts induced by the dipole-dipole interactions are negligible. We shall come back to this point in Sec. VI.

Let us therefore assume for the moment that during the interaction with the laser pulse the effects of dissipative spontaneous emission and dispersive dipole-dipole interactions are small, as compared to the effects of the coherent driving laser. We can then substitute the product of the electric field operator and the absolute value of the electronic transition dipole moment by

$$d\vec{\mathcal{E}}^{(+)} \to \frac{\Omega}{2}\sum_{\mu}\int d\vec{k}\;\vec{\varrho}(\vec{k},\mu)e^{i\vec{k}\cdot\vec{R}-ickt}, \tag{3}$$

where Ω is the peak Rabi frequency of the laser pulse. The function $\vec{\varrho}(\vec{k},\mu)$ describes a $(\vec{k},\mu)$-dependent envelope of the laser pulse. We assume that the pulse has the form of a plane wave packet moving in the $\vec{k}_L$ direction with a central frequency ω_L and a linear polarization $\vec{\epsilon}_L$, so that

$$d\vec{\mathcal{E}}^{(+)} \to \frac{\Omega}{2}\vec{\epsilon}_L\mathcal{T}[\gamma_L(t-\vec{k}_L\cdot\vec{R}/\omega_L)]e^{i\vec{k}_L\cdot\vec{R}-i\omega_Lt}. \tag{4}$$

Here, $\mathcal{T}(\gamma_Lt)$ is the temporal envelope of the pulse; it is chosen to be real and assumed to have a bell shape with a maximum at $t=0$ equal to 1.

Note that to obtain Eq. (4), the $(\vec{k},\mu)$-dependent envelope $\vec{\varrho}(\vec{k},\mu)$ must change on a scale of momenta of the order of $\gamma_L/c \simeq 10-300$ m^{-1}. On the other hand, the characteristic scale on which the matrix elements $\eta_{\vec{n}\vec{m}}(\vec{k})$ change, δk is of the order of $1/a \simeq 10^5$ m^{-1} for low n [13]. As we go to higher n's, δk scales as $1/\sqrt{n}$, so it becomes $\sim 10^3$ m^{-1} for the highest energy levels that are still available in the trap. Since $\delta k \gg \gamma_L/c$ for all γ_L in question, we may thus safely substitute $\vec{k}$ by $\vec{k}_L$ inside $\eta_{\vec{n}\vec{m}}(\vec{k}_L)$. With this substitution, using Eq. (3) and Eq. (4), the Hamiltonian (1) becomes

$$\mathcal{H} = \sum_{\vec{n}}\omega^g_{\vec{n}}g^\dagger_{\vec{n}}g_{\vec{n}} + \sum_{\vec{m}}(\omega^e_{\vec{m}}+\omega_0)\vec{e}^{\,\dagger}_{\vec{m}}\vec{e}_{\vec{m}} + \frac{\Omega}{2}\mathcal{T}(\gamma_Lt)\Big[\exp(i\omega_Lt)\sum_n g^\dagger_{\vec{n}}\vec{\epsilon}_L\cdot\vec{f}_n + \text{H.c.}\Big], \tag{5}$$

where we have introduced a new notation for the annihilation and creation of wave packets of excited states which originate from the $\vec{n}$th state of the ground state potential,

$$\vec{f}_{\vec{n}} = \sum_{\vec{m}}\eta_{\vec{n}\vec{m}}(\vec{k}_L)\vec{e}_{\vec{m}}. \tag{6}$$

Note that these annihilation and creation operators describe independent wave packets, i.e., they obey the standard bosonic commutation relations $[f^q_{\vec{n}}, f^{q'\dagger}_{\vec{n}'}] = \delta_{\vec{n}\vec{n}'}\delta_{qq'}$, with $q,q' = x,y,z$ enumerating the components of the vectors $\vec{f}_{\vec{n}}$ and $\vec{f}^{\,\dagger}_{\vec{n}'}$. Moreover, the energies $\omega_{\vec{m}}$ vary very slowly for the states in question and, therefore, for each of the wave packets $\vec{f}_{\vec{n}}$, $\vec{f}^{\,\dagger}_{\vec{n}}$, their energy can be approximated by $\omega^g_{\vec{n}}+\omega_0+k_L^2/(2M)$. This assumption is equivalent to the statement that the atomic wave packets in the excited state potential will not experience much coherent oscillation or diffusion (i.e., are in a sense frozen in shape) within the duration of the laser pulse ($\tau_L \ll 1/\omega_t$). Furthermore, $\omega^g_{\vec{n}}$'s are of the order of 10 Hz for low n, and of the order of, say, 10^5 Hz for the highest accessible states in the trap [13]. Compared with γ_L, they can be safely neglected.

The Heisenberg equations that follow from the Hamiltonian (5) now become linear. Thus at resonance, $\omega_L \approx \omega_0 + k_L^2/(2M)$, and in the rotating frame in which $g_{\vec{n}} \to e^{-i\omega^g_{\vec{n}}t}g_{\vec{n}}$, $\vec{f}_{\vec{n}} \to e^{-i(\omega^g_{\vec{n}}+\omega_L)t}\vec{f}_{\vec{n}}$, they take a particularly simple form:

$$\dot{g}_{\vec{n}}(t) = -i\frac{\Omega}{2}\mathcal{T}(\gamma_Lt)\vec{\epsilon}_L\cdot\vec{f}_{\vec{n}}(t), \tag{7}$$

$$\vec{\epsilon}_L\cdot\dot{\vec{f}}_{\vec{n}}(t) = -i\frac{\Omega}{2}\mathcal{T}(\gamma_Lt)g_{\vec{n}}(t). \tag{8}$$

These equations may be easily solved analytically for any pulse envelope

$$g_{\vec{n}}(t) = g_{\vec{n}}(-\infty)\cos\big[A(t)\big] - i\vec{\epsilon}_L\cdot\vec{f}_{\vec{n}}(-\infty)\sin\big[A(t)\big], \tag{9}$$

$$\vec{\epsilon}_L\cdot\vec{f}_{\vec{n}}(t) = -ig_{\vec{n}}(-\infty)\sin\big[A(t)\big] + \vec{\epsilon}_L\cdot\vec{f}_{\vec{n}}(-\infty)\cos\big[A(t)\big], \tag{10}$$

with $A(t) = (\Omega/2)\int_{-\infty}^t\mathcal{T}(\gamma_Lt')dt'$. All other components of $\vec{f}_{\vec{n}}$ remain unchanged in this process. The physical picture is now the following: each of the $\vec{n}$ levels of the ground state oscillator (when populated) creates an independent wave packet $\vec{f}_{\vec{n}}$ which is a superposition of the excited state wave functions. The population oscillates coherently between the $\vec{n}$th ground state and the corresponding excited state wave packet. The system behaves as if it consists of a set of independent two-level atoms coherently driven by the laser pulse. If the area of the pulse is a multiple of 2π the system will be left in the same state after the pulse is gone as it was before it came. Obviously, as $|\vec{n}|$ increases, the approximations we have made become more problematic, but they should hold very well for the lowest available 10^4 states of the ground state potential [13].

Note that the relations

$$\vec{f}_{\vec{n}} = \sum_{\vec{m}} \eta_{\vec{n}\vec{m}}(\vec{k}_L)\vec{e}_{\vec{m}}, \tag{11}$$

$$\vec{f}_{\vec{n}}^{\,\dagger} = \sum_{\vec{m}} \left[\eta_{\vec{n}\vec{m}}(\vec{k}_L)\right]^* \vec{e}_{\vec{m}}^{\,\dagger}, \tag{12}$$

imply the inverse relations

$$\sum_{\vec{n}} \vec{f}_{\vec{n}} \left[\eta_{\vec{n}\vec{m}}(\vec{k}_L)\right]^* = \vec{e}_{\vec{m}}, \tag{13}$$

$$\sum_{\vec{n}} \vec{f}_{\vec{n}}^{\,\dagger} \eta_{\vec{n}\vec{m}}(\vec{k}_L) = \vec{e}_{\vec{m}}^{\,\dagger}. \tag{14}$$

The above expressions follow from the sum rules

$$\sum_{\vec{n}} \left[\eta_{\vec{n}\vec{m}}(\vec{k}_L)\right]^* \eta_{\vec{n}\vec{m}'}(\vec{k}_L) = \delta_{\vec{m}\vec{m}'}, \tag{15}$$

$$\sum_{\vec{m}} \left[\eta_{\vec{n}\vec{m}}(\vec{k}_L)\right]^* \eta_{\vec{n}'\vec{m}}(\vec{k}_L) = \delta_{\vec{n}\vec{n}'}. \tag{16}$$

They will allow us to express solutions for $g_{\vec{n}}(t)$ and $\vec{e}_{\vec{m}}(t)$ as given above in Eqs. (9) and (10) (and their conjugates) uniquely in terms of $g_{\vec{n}}(-\infty)$, $\vec{e}_{\vec{m}}(-\infty)$, etc.

Of course, in reality the atoms will scatter photons, since γ is nonzero. The resonance fluorescence (RF) from a single atom driven by a short pulse has been studied by Rzążewski and Florjańczyk [17]. They have shown that the RF spectrum in such a case consists of $2K-1$ peaks, provided the pulse area is $2\pi K$. Physically, multiple splitting results from temporal interference effects, as photons emitted during the interaction with the pulse interfere with each other. These results were then generalized to include nonzero detunings, dissipation, and various pulse shapes (hyperbolic secant, exponential pulses, chirped pulses, etc.) [18]. The total number of photons emitted per atom in such a process $N_{\rm tot}$ was shown to be typically of the order of γ/γ_L, i.e. $\ll 1$.

III. SPECTRUM OF THE SCATTERED LIGHT

Before we turn to the calculation of the properties of the light scattered from the system, we have to specify the initial conditions for Eqs. (9) and (10) at $t=-\infty$. For the class A model, we assume that initially the ground state energy levels were populated in accordance with a Bose-Einstein distribution (BED) for noninteracting atoms in the harmonic well. The mean number of atoms in the $\vec{n}$th level at $t=-\infty$ is therefore

$$N_{\vec{n}} = \langle g_{\vec{n}}^\dagger g_{\vec{n}}\rangle = {\rm z}e^{-\beta\omega_{\vec{n}}}/(1-{\rm z}e^{-\beta\omega_{\vec{n}}}), \tag{17}$$

where $\beta = 1/kT$, and z is the fugacity. The relation $\sum_{\vec{n}} N_{\vec{n}} = N$ determines z as a function of β and N. Below the critical temperature T_c, and in the appropriately defined thermodynamic limit [19,20], ${\rm z}=1$ and N_0 becomes extensive. In all of the numerical examples presented below we shall, however, use BED for finite N which, rigorously speaking, exhibits a "smoothed" phase transition only. Some properties of BED for finite N are illustrated in Fig. 1, where we plot the temperature $\beta\omega_t$ as a function of the ground state occupation N_0 for the finite system we are considering.

After specifying initial conditions, we can calculate the spectrum of scattered photons. Thus, using the Hamiltonian (1), we derive the Heisenberg equation for the photon annihilation operator,

$$\dot{a}_{\vec{k}\mu} = -icka_{\vec{k}\mu} - i\varrho(k)\sum_{\vec{n},\vec{m}} g_{\vec{n}}^\dagger \vec{e}_{\vec{m}}\cdot\vec{\epsilon}_{\vec{k}\mu}\eta_{\vec{n}\vec{m}}(\vec{k}), \tag{18}$$

and a Hermitian conjugated one for $a_{\vec{k}\mu}^\dagger$. These equations are now solved perturbatively with respect to the atom-photon field coupling $\varrho(k)$. The formal solution of Eqs. (18) is

$$a_{\vec{k}\mu}(t) = e^{-ickt}a_{\vec{k}\mu}(-\infty) - i\varrho(k)\sum_{\vec{n},\vec{m}}\eta_{\vec{n}\vec{m}}(\vec{k}) \times \int_{-\infty}^{t} dt' e^{-ick(t-t')}\vec{\epsilon}_{\vec{k}\mu}\cdot\vec{e}_{\vec{m}}(t')g_{\vec{n}}^\dagger(t'). \tag{19}$$

The perturbative solution is then obtained by inserting

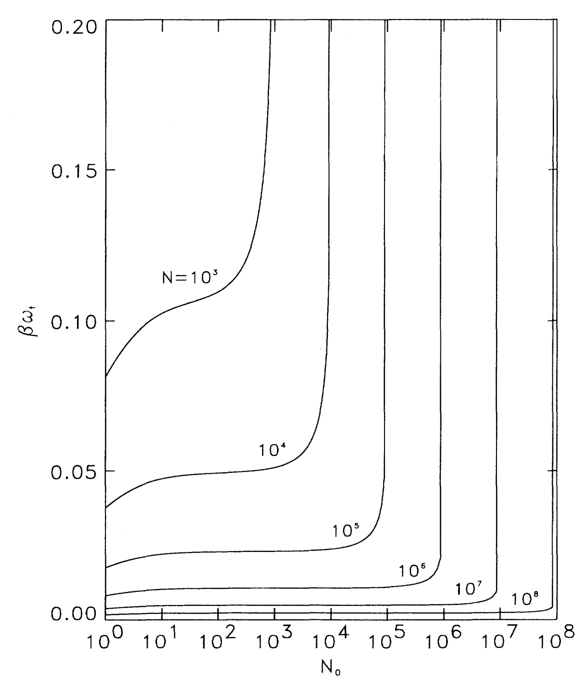

FIG. 1. The dependence of $\beta\omega_t$ on the ground state occupation N_0 for various values of N.

$g_{\vec{n}}(t)$, $\vec{e}_{\vec{m}}(t)$ constructed from Eqs. (9) and (10), (11) and (12), and (13) and (14).

The total spectrum of scattered photons is defined as

$$C(\vec{k},\mu) = \lim_{t\to\infty} \langle a^\dagger_{\vec{k}\mu}(t) a_{\vec{k}\mu}(t)\rangle, \tag{20}$$

and can be divided into coherent and incoherent parts,

$$C(\vec{k},\mu) = C_{\rm coh}(\vec{k},\mu) + C_{\rm in}(\vec{k},\mu). \tag{21}$$

The coherent part is, as in the single-atom case, proportional to the modulus squared of the Fourier transform of the mean atomic polarization. The incoherent part originates from the quantum fluctuations of the atomic polarization. Although in experiments only the total spectrum can be measured, the division into coherent and incoherent parts is meaningful since they have significantly different angular characteristics, as we show below. The total spectrum takes the form

$$C(\vec{k},\mu) = |\varrho(k)|^2 |\vec{\epsilon}_L\cdot\vec{\epsilon}_{\vec{k}\mu}|^2 \sum_{\vec{n}_1,\vec{m}_1,\vec{n}_2,\vec{m}_2} [\eta_{\vec{n}_1\vec{m}_1}(\vec{k})]^* \eta_{\vec{n}_2\vec{m}_2}(\vec{k}) \sum_{\vec{n}'_1,\vec{n}'_2} \eta_{\vec{n}'_1\vec{m}_1}(\vec{k}_L)[\eta_{\vec{n}'_2\vec{m}_2}(\vec{k}_L)]^*$$
$$\times \int_{-\infty}^{\infty} dt_1 \int_{-\infty}^{\infty} dt_2 e^{-i(ck-\omega_L)t_1} e^{i(ck-\omega_L)t_2} \langle \vec{f}^\dagger_{\vec{n}'_1}(t_1)\cdot\vec{\epsilon}_L g_{\vec{n}_1}(t_1) g^\dagger_{\vec{n}_2}(t_2) \vec{f}_{\vec{n}'_2}(t_2)\cdot\vec{\epsilon}_L\rangle. \tag{22}$$

In the perturbative limit, we now insert the solutions of Eqs. (9) and (10) into Eq. (22). At $t=-\infty$, the Heisenberg picture coincides with the Schrödinger picture, so that we omit in the following the explicit time dependence of the operators at $t=-\infty$. Since initially all atoms are in the ground electronic state, we obtain

$$\langle \vec{f}^\dagger_{\vec{n}'_1}(t_1)\cdot\vec{\epsilon}_L g_{\vec{n}_1}(t_1) g^\dagger_{\vec{n}_2}(t_2)\vec{f}_{\vec{n}'_2}(t_2)\cdot\vec{\epsilon}_L\rangle = \langle g^\dagger_{\vec{n}'_1} g_{\vec{n}_1} g^\dagger_{\vec{n}_2} g_{\vec{n}'_2}\rangle \sin[A(t_1)]\cos[A(t_1)]\sin[A(t_2)]\cos[A(t_2)]$$
$$+\langle g^\dagger_{\vec{n}'_1}\vec{\epsilon}_L\cdot\vec{f}_{\vec{n}_1}\vec{\epsilon}_L\cdot\vec{f}^\dagger_{\vec{n}_2} g_{\vec{n}'_2}\rangle \sin^2[A(t_1)]\sin^2[A(t_2)], \tag{23}$$

where the expectation values $\langle\,\rangle$ with respect to the BED remain to be evaluated.

We define two quantities that describe single-atom response [17,18]. The single-atom spectrum can also be written as a sum of coherent and incoherent parts,

$$S(\varpi) = S_{\rm coh}(\varpi) + S_{\rm in}(\varpi), \tag{24}$$

with $\varpi = (ck-\omega_L)/\gamma_L$, and

$$S_{\rm coh,in}(x) = \frac{3}{8\pi^2}\frac{\gamma}{\gamma_L^2}\frac{c}{k_0^2}(\vec{\epsilon}_{\vec{k}\mu}\cdot\vec{\epsilon}_L)^2 W_{\rm coh,in}(x). \tag{25}$$

The dimensionless spectra $W_{\rm coh,in}(x)$ are defined as

$$W_{\rm coh}(x) = \gamma_L^2\left|\int_{-\infty}^{\infty} e^{-ix\gamma_L t'}\cos[A(t')]\sin[A(t')]dt'\right|^2, \tag{26}$$

$$W_{\rm in}(x) = \gamma_L^2\left|\int_{-\infty}^{\infty} e^{-ix\gamma_L t'}\sin^2[A(t')]dt'\right|^2. \tag{27}$$

The analytic formulas for the single-atom spectra $W_{\rm coh,in}(\varpi)$ for a variety of laser pulse shapes can be found in Refs. [17,18]. For instance, for a hyperbolic secant pulse $1/\cosh(\gamma_L t)$ of area 2π [21],

$$W_{\rm coh}(x) = \pi x^2/\cosh^2(\pi x/2), \tag{28}$$
$$W_{\rm in}(x) = \pi x^2/\sinh^2(\pi x/2). \tag{29}$$

In the following, we shall concentrate on this case only, and use the above expressions in numerical calculations. The results that we shall present for pulses of $2\pi K$ area are universal, however, and only weakly depend on a particular pulse shape.

Using the relation

$$\sum_{\vec{m}} [\eta_{\vec{n}'\vec{m}}(\vec{k})]^* \eta_{\vec{n}\vec{m}}(\vec{k}_L) = \eta_{\vec{n}\vec{n}'}(\vec{k}_L - \vec{k}), \tag{30}$$

we obtain

$$C(\vec{k},\mu) = |\varrho(k)|^2|\vec{\epsilon}_L\cdot\vec{\epsilon}_{\vec{k}\mu}|^2 \times \sum_{\vec{n}_1,\vec{n}_2,\vec{n}'_1,\vec{n}'_2}[\eta_{\vec{n}_1\vec{n}'_1}(\vec{k}-\vec{k}_L)]^*\eta_{\vec{n}_2\vec{n}'_2}(\vec{k}-\vec{k}_L) \times\frac{1}{\gamma_L^2}\Big[\langle g^\dagger_{\vec{n}'_1} g_{\vec{n}_1} g^\dagger_{\vec{n}_2} g_{\vec{n}'_2}\rangle W_{\rm coh}(\varpi) + \langle g^\dagger_{\vec{n}'_1}\vec{\epsilon}_L\cdot\vec{f}_{\vec{n}_1}\vec{\epsilon}_L\cdot\vec{f}^\dagger_{\vec{n}_2} g_{\vec{n}'_2}\rangle W_{\rm in}(\varpi)\Big]. \tag{31}$$

Making use of the properties of the BED, we get

$$\langle g^\dagger_{\vec{n}'_1} g_{\vec{n}_1} g^\dagger_{\vec{n}_2} g_{\vec{n}'_2}\rangle = \delta_{\vec{n}'_1\vec{n}_1}N_{\vec{n}_1}\delta_{\vec{n}'_2\vec{n}_2}N_{\vec{n}_2} + \delta_{\vec{n}'_1\vec{n}_1}\delta_{\vec{n}'_2\vec{n}_2}\delta_{\vec{n}_1\vec{n}_2}(\langle(g^\dagger_{\vec{n}_1}g_{\vec{n}_1})^2\rangle - N^2_{\vec{n}_1}) + \delta_{\vec{n}_1\vec{n}_2}\delta_{\vec{n}'_1\vec{n}'_2}N_{\vec{n}'_1}(1+N_{\vec{n}_1})|_{\vec{n}_2\neq\vec{n}'_2}, \tag{32}$$

and

$$\langle g^\dagger_{\vec{n}'_1}\vec{\epsilon}_L\cdot\vec{f}_{\vec{n}_1}\vec{\epsilon}_L\cdot\vec{f}^\dagger_{\vec{n}_2}g_{\vec{n}'_2}\rangle=\delta_{\vec{n}_1\vec{n}_2}\delta_{\vec{n}'_1\vec{n}'_2}N_{\vec{n}'_1}. \qquad (33)$$

Inserting the above expressions in Eq. (31), and performing tedious but elementary calculations we finally obtain analytic expressions for the spectra. In particular, the coherent part takes the following form:

$$C_{\rm coh}(\vec{k},\mu)=S_{\rm coh}(\varpi)\left|\sum_{\vec{n}}N_{\vec{n}}\eta_{\vec{n}\vec{n}}(\vec{k}-\vec{k}_L)\right|^2, \qquad (34)$$

The analytic expression for the coherent spectrum is derived in Appendix B. The incoherent part of the spectrum, on the other hand, can be expressed as

$$C_{\rm in}(\vec{k},\mu)=S_{\rm coh}(\varpi)\sum_{\vec{n}}\delta N^2_{\vec{n}}\left|\eta_{\vec{n}\vec{n}}(\vec{k}-\vec{k}_L)\right|^2+S_{\rm coh}(\varpi)\sum_{\vec{n}}\sum_{\vec{n}'\neq\vec{n}}N_{\vec{n}}(1+N_{\vec{n}'})\left|\eta_{\vec{n}\vec{n}'}(\vec{k}-\vec{k}_L)\right|^2+NS_{\rm in}(\varpi). \qquad (35)$$

It is worth noting that the incoherent spectrum (35) consists of three parts coming from (i) quantum dispersion of the occupation numbers $\delta N^2_{\vec{n}}=\langle(g^\dagger_{\vec{n}}g_{\vec{n}})^2\rangle-\langle g^\dagger_{\vec{n}}g_{\vec{n}}\rangle^2$, (ii) processes of creation of the nth wave packet accompanied by annihilation of the $\vec{n}'$th one for $\vec{n}\neq\vec{n}'$, and (iii) the single atom incoherent spectrum. Each of these contributions can be evaluated analytically (see Appendixes C and D). Obviously, both coherent and incoherent spectra reflect quantum statistical properties of atoms, since they depend on $N_{\vec{n}}$'s, which are described by Bose-Einstein and Fermi-Dirac distributions for bosons and fermions, respectively. Additionally, the first two terms in Eq. (35) for the incoherent spectrum depend explicitly on the statistical properties of atoms through $\delta N^2_{\vec{n}}$ and the factor $(1+N_{\vec{n}'})$, which is a final state bosonic degeneracy enhancement for the Raman process involved. The later factor is replaced by $(1-N_{\vec{n}'})$ for fermionic atoms [22].

The total number of emitted photons can be obtained by integrating the spectrum,

$$N_{\rm tot}=\sum_\mu\int d\vec{k}\;C(\vec{k},\mu). \qquad (36)$$

Obviously, $N_{\rm tot}$ can also be divided into coherent and incoherent parts. By fixing the direction of $\vec{k}$ and integrating over the azimuthal angle φ one can also define an angular distribution of photons $dN_{\rm tot}(\theta)$ [and, correspondingly, $dN_{\rm coh}(\theta)$ and $dN_{\rm in}(\theta)$]

$$dN_{\rm tot}(\theta)=dN_{\rm coh}(\theta)+dN_{\rm in}(\theta)=\sin(\theta)d\theta\sum_\mu\int_0^{2\pi}d\varphi\int k^2dk\;C(\vec{k},\mu), \qquad (37)$$

where θ is the angle between $\vec{k}$ and $\vec{k}_L$. Analogously, one can define an integrated spectrum by fixing $|\vec{k}|$, and integrating the spectrum over the full solid angle.

IV. DISCUSSION OF THE SPECTRUM

The coherent spectrum is proportional to N^2, whereas the incoherent part is typically of the order of N only. This means that when the number of atoms in the trap is large, one expects that the number of coherently scattered photons $N_{\rm coh}$ will dominate over the number of incoherent ones, $N_{\rm in}$.

As shown in Appendix B, the coherent spectrum Eq. (21) can be simplified to the following form:

$$C_{\rm coh}(\vec{k},\mu)=S_{\rm coh}(\varpi)\left|\sum_{l=1}^\infty\frac{{\rm z}^l}{(1-e^{-l\beta\omega_t})^3}\times\exp\left[-\tfrac{1}{2}(\vec{k}-\vec{k}_L)^2a^2\coth(l\beta\omega_t/2)\right]\right|^2. \qquad (38)$$

Strictly speaking, as $N\to\infty$ Eq. (38) can be used only for $T>T_c$. For finite N it can be, in principle, used at all temperatures, but as $T\to0$ the convergence of the series in Eq. (38) becomes very slow.

Note that according to Eq. (38) the range of possible scattering angles is determined by the size of the trap and a temperature-dependent factor that results from destructive interference of different $\vec{n}$ terms in the sum entering Eq. (34). As T grows, ${\rm z}\to0$, and only the first term in the sum in Eq. (38) remains relevant. We obtain, then,

$$C_{\rm coh}(\vec{k},\mu)=S_{\rm coh}(\varpi)N^2\exp\left[-2(\vec{k}-\vec{k}_L)^2a^2/\beta\omega_t\right]. \qquad (39)$$

For $T\simeq10\;\mu K$, $\beta\omega_t\simeq5\times10^{-5}$ and the scattering will occur practically in the forward direction and will cover only a tiny solid angle with half angle $\leq1.0\times10^{-4}$. The total number of coherently scattered photons becomes, then,

$$N_{\rm coh}=\frac{3\pi^{3/2}}{16}\frac{\gamma}{\gamma_L}N^2\left(\frac{\beta\omega_t}{2a^2k_L^2}\right)^{5/2}\left(\frac{\omega_L}{\gamma_L}\right)^3. \qquad (40)$$

In deriving Eq. (40) one has to take into account the fact that the single atom spectrum $W_{\rm coh}(x)$ behaves as $\propto x^2$ for $x\to0$.

For $N=10^8$, $a=10\;\mu$m, $N_{\rm coh}$ will be of the order of 2% of N for a 100 ps pulse and 2×10^{-4}% of N for a 10 ps one. As we see, our theory is self-consistent in this high temperature limit, since $N_{\rm coh}\ll N$.

As T decreases, more and more terms in the sum over l in Eq. (38) contribute and more and more photons are emitted. The critical value of $\beta\omega_t$ for BEC may be estimated to be $(\beta\omega_t)_c\simeq(1.202/N)^{1/3}\simeq2\times10^{-3}$ [19,20]. Amazingly, numerical analysis of the expression (38) indicates that for temperatures higher than (even close to)

T_c, only a few terms in the series (38) are relevant. In other words, the high temperature approximation breaks down only very close to the critical point. In this case, the the single term on the right-hand side (rhs) of the estimate (40) should be replaced by a sum of a few similar terms that differ by numerical factors of the order of one. Therefore, to get a rough estimate we may still use the expression (40) and obtain $N_{\rm coh} > N$ for a 100 ps pulse and $N_{\rm coh} = 4\%N$ for a 10 ps pulse for T greater than (even close to) T_c. As we see, our theory is beyond the limits of its validity for 100 ps pulses. However, we point out the very strong dependence on a in Eq. (40); for flatter potentials with larger a, the validity of the theory can be easily extended into the regime of nanosecond pulses. For the same reasons as mentioned above [i.e., rapid convergence of the series in Eq. (38)], for T greater than, even very close to, T_c, most of the coherently scattered photons will be emitted in the forward direction. Thus, detection of scattered photons is very difficult since, in practice, they cannot be distinguished from the laser photons.

Similar conclusions hold also for the incoherent part of the spectrum at high temperatures. As shown in Appendix C, the incoherent spectrum can be represented as

$$C_{\rm in}(\vec{k},\mu) = S_{\rm coh}(\varpi)\sum_{l_1,l_2=1}^{\infty}\frac{z^{l_1+l_2}}{[1-e^{-(l_1+l_2)\beta\omega_t}]^3} \times\exp\left[-(\vec{k}-\vec{k}_L)^2a^2 f(\beta,l_1,l_2)\right] +NS_{\rm coh}(\varpi)+NS_{\rm in}(\varpi), \qquad (41)$$

with

$$f(\beta,l_1,l_2) = \frac{(1-e^{-l_1\beta\omega_t})(1-e^{-l_2\beta\omega_t})}{1-e^{-(l_1+l_2)\beta\omega_t}}. \qquad (42)$$

It can be proven that for arbitrary $l_1, l_2 \geq 1$ and β,

$$0 < f(\beta,l_1,l_2) < 1. \qquad (43)$$

As T grows, only the term corresponding to $l_1 = l_2 = 1$ contributes to the sum in Eq. (41), and the incoherent spectrum becomes

$$C_{\rm in}(\vec{k},\mu) = S_{\rm coh}(\varpi)N^2(\beta\omega_t/2)^3 \times\exp\left[-\tfrac{1}{2}(\vec{k}-\vec{k}_L)^2a^2\beta\omega_t\right] +NS_{\rm coh}(\varpi)+NS_{\rm in}(\varpi). \qquad (44)$$

Numerical analysis of the expression (41) leads to a similar conclusion as in the case of the coherent spectrum. For T greater than (even close to) T_c, only a few terms in the series on the rhs of Eq. (41) are relevant, and the high temperature expansion, works amazingly well. Using this expansion we can estimate that for T greater than but close to T_c, i.e., for $\beta\omega_t \simeq 2\times 10^{-3}$ and 300 ps pulses, the number of incoherently scattered photons is much less than N. Note, however, that they may be emitted into the full solid angle 4π, since now the phase matching introduces a small factor $\beta\omega_t$ in the exponent.

The situation dramatically changes when $T < T_c$. The spectrum will contain a new term arising from the condensate. Assuming that on average there are N_0 atoms occupying the lowest energy state with $\vec{n} = (0,0,0)$, we obtain for the coherent part

$$C_{\rm coh}^{\rm BEC}(\vec{k},\mu) = S_{\rm coh}(\varpi)N_0^2\exp\left[-(\vec{k}-\vec{k}_L)^2a^2\right]. \qquad (45)$$

As we would expect, the coherent scattering now covers a much larger solid angle with half angle $\sim 1.0\times 10^{-2}$. At a distance of 1 m from the trap the scattered photons will be about 1 cm off the optical axis. The total number of such photons also grows dramatically as N_0 grows and T becomes smaller. We obtain

$$N_{\rm coh}^{\rm BEC} = N_0^2\frac{\gamma}{\gamma_L}\frac{1}{2k_L^2a^2}. \qquad (46)$$

The validity of the theory requires that $N_{\rm coh} \ll N_0$. For a 100 ps pulse this condition holds provided $N_0 \leq 10^7$. For $N = 10^8$, N_0 will in fact reach this value just below the critical temperature $[N_0/N = 1-(T/T_c)^3]$. About 10^4 photons will be scattered coherently into the solid angle $4\pi/(k_La)$ as $(1-T/T_c)$ becomes $\simeq 3\times 10^{-3}$. For 10 ps pulses, our theory is valid even if all the atoms were in the condensate.

The incoherent spectrum, on the other hand, in the presence of a condensate includes the term

$$C_{\rm in}^{\rm BEC}(\vec{k},\mu) = -(N_0+1)S_{\rm coh}(\varpi)\exp\left[-(\vec{k}-\vec{k}_L)^2a^2\right] +(2N_0+1)S_{\rm coh}(\varpi)+NS_{\rm in}(\varpi). \qquad (47)$$

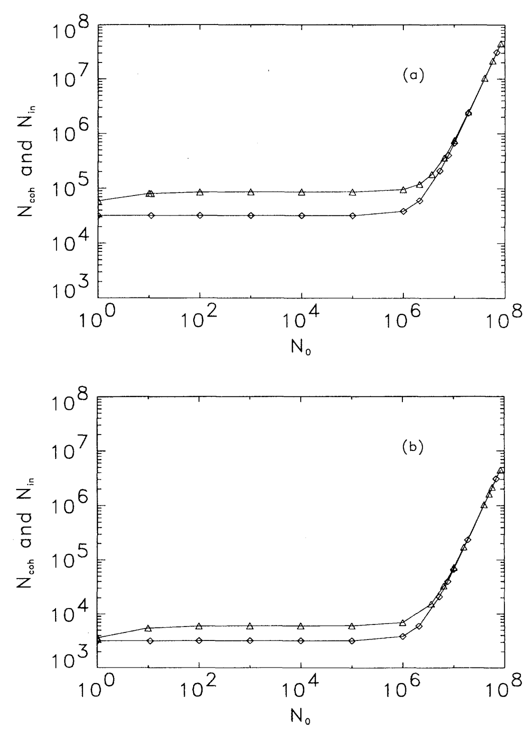

FIG. 2. The dependence of the number of coherently (triangles) and incoherently (diamonds) scattered photons on the condensate occupation N_0 for (a) $\tau_L = 1/\gamma_L = 100$ (ps), and (b) $\tau_L = 1/\gamma_L = 10$ (ps) with $N = 10^8$.

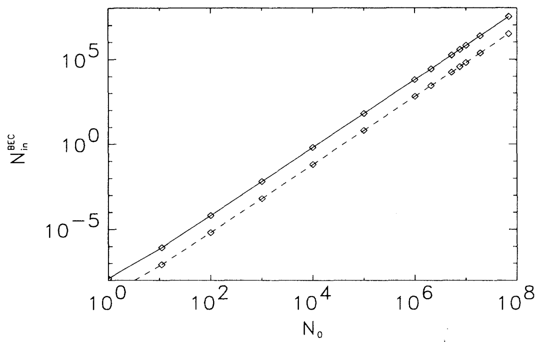

FIG. 3. The number of incoherently scattered photons due to the fluctuations of the condensate occupation $\delta N_0^2 = N_0(N_0+1)$ for $\tau_L = 1/\gamma_L = 100$ (ps) (solid line) and $\tau_L = 1/\gamma_L = 10$ (ps) (dashed line). Diamonds denote the calculated points. For weakly interacting gases, this contribution should be subtracted from the results displayed in Fig. 2.

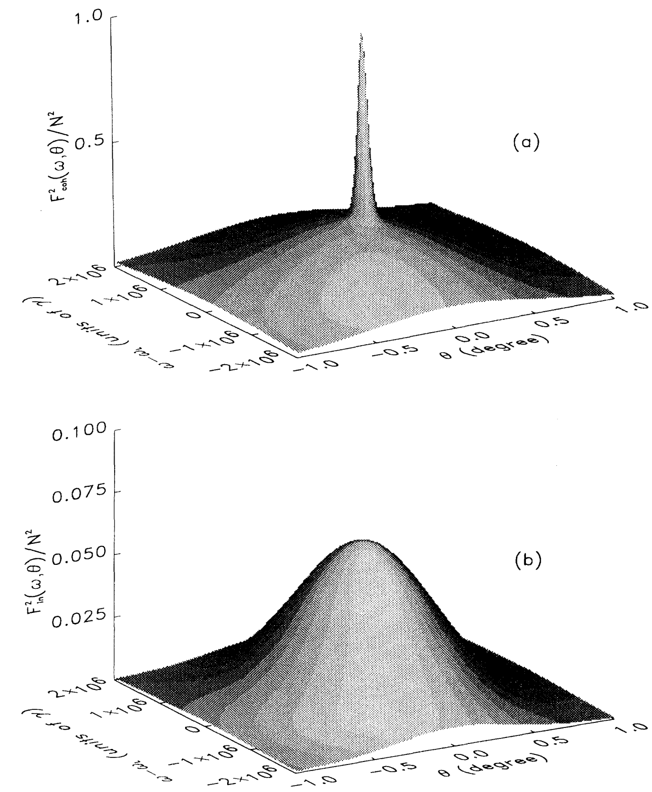

FIG. 4. The angular and spectral dependence of the scattering amplitude squared for (a) coherent scattering as given by Eq. (38), and (b) incoherent scattering as given by Eq. (41), for $N_0 = 5\times 10^7$ with $N = 10^8$.

This expression is derived under the assumption that the fluctuations of N_0 correspond to those of the coherent state, i.e., $\delta N_0^2 = N_0$ [24]. The number of incoherently scattered photons due to the condensate remains much smaller than N in the whole regime of parameters considered.

The above analysis is well supported by our numerical findings. In Fig. 2 we present results concerning the total number of coherently and incoherently scattered photons calculated according to Eq. (38) and Eq. (41), respectively. In the limit where N_0 is a significant fraction of the total number of the atoms, we notice that the number of incoherently scattered photons also shows a quadratic dependence on N_0, since, for class A models as used in Eqs. (38) and (41), strictly speaking, $\delta N_0^2 = N_0(N_0+1)$ because a Bose-Einstein distribution with no interaction is used. According to the discussion above, a more appropriate approach would be to set $\delta N_0^2 = N_0$ [24]. In other words, a correction has to be made whenever interactions between atoms exist. In Fig. 3, we plot the number of incoherently scattered photons due to fluctuations of the condensate occupation using the expression $\delta N_0^2 = N_0(N_0+1)$ which is used in calculating Eq. (41) rather than $\delta N_0^2 = N_0$. Comparing with the results presented in Fig. 2, we see that those photons represent the dominant contribution to the incoherent scattering that should be excluded in realistic interacting systems. Therefore, for the two cases considered, scattering is dominated by coherent events ($N_{\rm coh} \gg N_{\rm in}$), and the perturbative calculation is self-consistent, since $N_{\rm coh} + N_{\rm in} \ll N$. We plot these quantities as a function of N_0 [which is equivalent to plotting the temperature dependence as given in Fig. 1]. In Fig. 4 we plot the coherent scattering phase-matching amplitude squared [from Eq. (B9)],

$$\mathcal{F}^2_{\rm coh}(\omega-\omega_L,\theta) = \left|\sum_{m=1}^{\infty} \frac{\mathrm{z}^m}{(1-e^{-m\beta\omega_t})^3}\exp\left[-\tfrac{1}{2}(\vec{k}-\vec{k}_L)^2a^2\coth(m\beta\omega_t/2)\right]\right|^2, \tag{48}$$

as well as the incoherent phase-matching amplitude squared [see Eqs. (41) and (D5)],

$$\mathcal{F}^2_{\rm in}(\omega-\omega_L,\theta) = \sum_{l_1,l_2=1}^{\infty} \frac{\mathrm{z}^{l_1+l_2}}{[1-e^{-(l_1+l_2)\beta\omega_t}]^3}\exp\left[-(\vec{k}-\vec{k}_L)^2a^2 f(\beta,l_1,l_2)\right]. \tag{49}$$

These quantities basically represent the collective spectral-spatial response of the atoms due to phase matching. For the coherent scattering, there are two basic features. The narrow peak in the middle of the surface results from the phase matching for the field scattered from noncondensed atoms. It has an angular width $\sim \sqrt{\beta\omega_t}/ka$, and a frequency width $\sim \sqrt{\beta\omega_t}(c/a)$. On the other hand, the broad overall background is due to

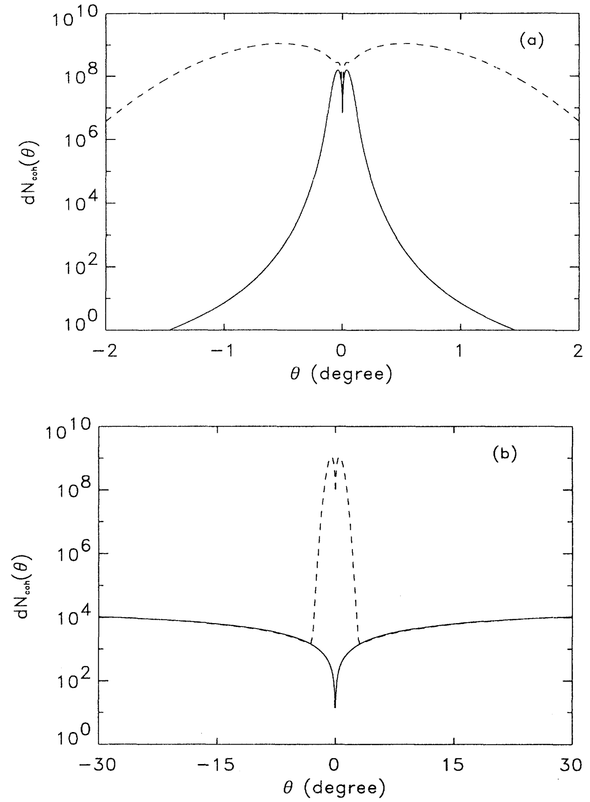

FIG. 5. The angular distributions of the scattered photons, for $N_0 = 10^3$ (solid line) and $N_0 = 5 \times 10^7$ (dashed line) with $N = 10^8$, (a) coherent scattering as from Eq. (38), and (b) incoherent scattering as from Eq. (41); $\tau_L = 100$ (ps).

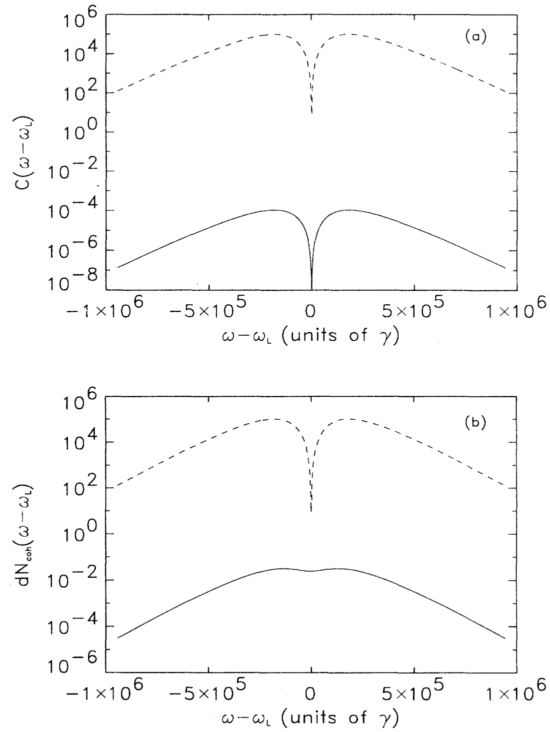

FIG. 6. The frequency spectrum for photons emitted at an angle $1/(k_L a)$ (with respect to the propagation axis of the laser pulse) calculated from Eqs. (38) and (41) for $N_0 = 10^3$ (solid line) and $N_0 = 5 \times 10^7$ (dashed line) with $N = 10^8$, (a) coherent scattering, and (b) incoherent scattering; $\tau_L = 100$ (ps).

the condensate and has an angular width $\sim 1/ka$, and a frequency width $\sim c/a$. Very similar conclusions hold for the incoherent scattering amplitude squared except that the angular distribution is now significantly broader. Note also that in Eq. (41) for the incoherent spectrum, two additional terms $NS_{\rm coh}(\varpi)$ and $NS_{\rm in}(\varpi)$ give rise to an extremely broad single atom dipole angular distribution. However, their contribution to the total number of scattered photons is small, $\sim N\gamma/\gamma_L$. In Fig. 5 we present a set of plots for the angular distributions of the scattered field, for high and low temperatures (above and below the condensation point). In Fig. 6 we present the frequency spectrum for photons emitted at an angle $1/(k_L a)$ with respect to the propagation axis of the laser pulse. In the parameter regime we are considering, the dominant contributing factor is $W_{\rm coh}(\varpi)$ for both coherent and incoherent spectra.

V. SQUEEZING SPECTRUM

Calculations of the squeezing properties of the scattered photons can be performed analogously to the calculation of the spectrum. First, we calculate the following auxiliary quantity:

$$\mathcal{M}(\vec{k},\mu) = \lim_{t\to\infty} \langle a^\dagger_{\vec{k}\mu}(t) a^\dagger_{\vec{k}\mu}(t)\rangle. \tag{50}$$

As before, we obtain

$$\mathcal{M}(\vec{k},\mu) = |\varrho(k)|^2 |\vec{\epsilon}_L \cdot \vec{\epsilon}_{\vec{k}\mu}|^2 \sum_{\vec{n}_1,\vec{n}_2,\vec{n}_1',\vec{n}_2'} [\eta_{\vec{n}_1\vec{n}_1'}(\vec{k}-\vec{k}_L)]^* \times [\eta_{\vec{n}_2\vec{n}_2'}(\vec{k}-\vec{k}_L)]^* \frac{1}{\gamma_L^2}\left[-\langle g^\dagger_{\vec{n}_1'} g_{\vec{n}_1} g^\dagger_{\vec{n}_2'} g_{\vec{n}_2}\rangle W_{\rm coh}(\varpi) + \langle g^\dagger_{\vec{n}_1'} \vec{\epsilon}_L \cdot \vec{f}_{\vec{n}_1} \vec{\epsilon}_L \cdot \vec{f}^\dagger_{\vec{n}_2'} g_{\vec{n}_2}\rangle W_{\rm sc}(\varpi)\right], \tag{51}$$

where

$$W_{\rm sc}(x) = \gamma_L^2 \int_{-\infty}^{\infty} e^{-ix\gamma_L t'} \sin^2\left[A(t')\right] dt' \times \int_{-\infty}^{\infty} e^{-ix\gamma_L t''} \cos^2\left[A(t'')\right] dt'' = -W_{\rm in}(x) + 2\pi\gamma_L \delta(x) \int_{-\infty}^{\infty} \sin^2\left[A(t')\right] dt'. \quad (52)$$

For a hyperbolic secant pulse of the area 2π, we have

$$W_{\rm sc}(x) = -W_{\rm in}(x) + 4\pi\delta(x). \quad (53)$$

Following steps analogous to those in the preceding section, we arrive at the final expression

$$\mathcal{M}(\vec{k},\mu) = \mathcal{M}_{\rm coh}(\vec{k},\mu) + \mathcal{M}_{\rm in}(\vec{k},\mu), \quad (54)$$

where the coherent part is

$$\mathcal{M}_{\rm coh}(\vec{k},\mu) = -S_{\rm coh}(\varpi)\Big|\sum_{\vec{n}}{}' N_{\vec{n}}\eta_{\vec{n}\vec{n}}(\vec{k}-\vec{k}_L)\Big|^2 = -C_{\rm coh}(\vec{k},\mu), \quad (55)$$

whereas the fluctuation part (which contributes to the squeezing spectrum) is

$$\mathcal{M}_{\rm in}(\vec{k},\mu) = -S_{\rm coh}(\varpi)\sum_{\vec{n}} \delta N_{\vec{n}}^2 \big|\eta_{\vec{n}\vec{n}}(\vec{k}-\vec{k}_L)\big|^2 - S_{\rm coh}(\varpi)\sum_{\vec{n}}\sum_{\vec{m}\neq\vec{n}} N_{\vec{n}}(N_{\vec{m}}+1)\big|\eta_{\vec{n}\vec{m}}(\vec{k}-\vec{k}_L)\big|^2 + N S_{\rm sc}(\varpi). \quad (56)$$

In Eq. (56) we have defined the corresponding single-atom squeezing spectrum as

$$S_{\rm sc}(x) = \frac{3}{8\pi^2}\frac{\gamma}{\gamma_L^2}\frac{c}{k_0^2}(\vec{\epsilon}_{\vec{k}\mu}\cdot\vec{\epsilon}_L)^2 W_{\rm sc}(x). \quad (57)$$

The squeezing properties of the scattered field can be measured in homodyne or heterodyne type measurements in which the scattered field is mixed with a strong coherent signal [25]. Photon counting measurements on the combined signal reflect the squeezing properties of the scattered field. In particular, since in the present case the coherent signal dominates over the incoherent one, a direct measurement of the photon statistics in the scattered light will also provide information about one particular quadrature of the field. These types of measurements would be difficult to implement for the case of short pulse scattering. But measurements based on direct interference of broadband squeezed pulses have been proposed recently [26].

In order to characterize squeezing properties of the scattered fields, we introduce a squeezing spectrum. We use the expression of the squeezing spectrum based on conventionally defined quadrature fields. In general, the two (Hermitian) quadratures fields can be defined as

$$x_1(\vec{k},\mu) = \frac{1}{2}(a_{\vec{k},\mu}e^{i\phi/2} + a^\dagger_{\vec{k},\mu}e^{-i\phi/2}), \quad (58)$$

$$x_2(\vec{k},\mu) = \frac{1}{2i}(a_{\vec{k},\mu}e^{i\phi/2} - a^\dagger_{\vec{k},\mu}e^{-i\phi/2}), \quad (59)$$

where $\phi/2$ denotes the quadrature phase relative to the local oscillator used in the homodyne-heterodyne measurement. The squeezing spectrum $C_{\rm sc}(\vec{k},\mu)$ is defined as the normal ordered variance of the quadrature field $x_1(\vec{k},\mu)$, and is given by

$$C_{\rm sc}(\vec{k},\mu) = \langle : x_1^2 : \rangle - \langle : x_1 : \rangle^2 = \frac{1}{2}\left[C_{\rm in}(\vec{k},\mu) + \cos(\phi)\mathcal{M}_{\rm in}(\vec{k},\mu)\right] = \frac{1}{2}\left[\left[1-\cos(\phi)\right]C_{\rm in}(\vec{k},\mu) + N\cos(\phi)\frac{3}{2\pi}\frac{\gamma}{\gamma_L^2}\frac{c}{k_0^2}(\vec{\epsilon}_{\vec{k}\mu}\cdot\vec{\epsilon}_L)^2\delta(\varpi)\right], \quad (60)$$

where $: x_1 :$ denotes the normal ordering of the field operators. The squeezing spectrum defined above determines also the Mandel Q parameter for each of the modes [27]. Negative value of the squeezing spectrum for a particular mode signals sub-Poissonian statistics and, equivalently, squeezing for photons of the corresponding momentum $\vec{k}$ and polarization μ.

We found that for any ϕ and $\varpi \neq 0$ the signal is mostly super-Poissonian. It may, however, exhibit a narrow range of sub-Poissonian behavior when $\cos(\phi)$ is negative. There are two interesting limiting cases of the expression (60). When $\phi = 0$, the scattered radiation is coherent at all frequencies except $\varpi = 0$, where it exhibits strong super-Poissonian behavior. When $\phi = \pi$ the scattered light is super-Poissonian at all frequencies except $\varpi = 0$, where it exhibits strong sub-Poissonian behavior. The case $\phi = \pi$ can be realized, for instance, if the strong coherent signal has the same phase as the coherent part of the scattered field [note the minus sign in Eq. (55)].

VI. CLASS C MODELS IN THE POSITION REPRESENTATION

In this section we first reformulate the theory for class A models in the position representation. This approach will allow us to extend the theory to class B or C models, i.e., to include effects of atom-atom interactions.

Under the approximations that we have made in Sec. II, the Hamiltonian describing the evolution of the system during the laser pulse becomes

$$\mathcal{H} = \sum_{\vec{n}} \omega_L \vec{f}_{\vec{n}}^{\,\dagger} \vec{f}_{\vec{n}} + \frac{\Omega}{2}\mathcal{T}(\gamma_L t)\Big[\exp(i\omega_L t)\sum_{n} g_{\vec{n}}^{\dagger}\vec{\epsilon}_L\cdot\vec{f}_{\vec{n}} + \text{H.c.}\Big]. \tag{61}$$

Note that we are considering here the quasiresonant case such that $\omega_L \approx \omega_0 + k_L^2/(2M)$. Also, the trap energies $\omega_{\vec{n}}^g$ and $\omega_{\vec{m}}^e$ do not enter Eq. (61). We may rewrite this Hamiltonian in the position representation by introducing the atomic annihilation fields

$$\Psi_g(\vec{R}) = \sum_{\vec{n}} g_{\vec{n}}\psi_{\vec{n}}^g(\vec{R}), \tag{62}$$

$$\vec{\Psi}_e(\vec{R}) = \sum_{\vec{m}} \vec{e}_{\vec{m}}\psi_{\vec{m}}^e(\vec{R}), \tag{63}$$

and their conjugates; the $\psi_{\vec{n}}^g(\vec{R})$, $\psi_{\vec{m}}^e(\vec{R})$ are the wave functions for the corresponding trap states. We also introduce the excited wave packets field

$$\vec{\Psi}_f(\vec{R}) = \sum_{\vec{n}} \vec{f}_{\vec{n}}\psi_{\vec{n}}^g(\vec{R}) = \exp(-i\vec{k}_L\cdot\vec{R})\vec{\Psi}_e(\vec{R}), \tag{64}$$

and its Hermitian conjugate.

The Hamiltonian (which is valid only within the duration of the pulse) becomes thus

$$\mathcal{H} = \int d\vec{R}\;\omega_L\vec{\Psi}_f^{\dagger}(\vec{R})\cdot\vec{\Psi}_f(\vec{R}) + \frac{\Omega}{2}\mathcal{T}(\gamma_L t) \times\Big[\exp(i\omega_L t)\int d\vec{R}\;\Psi_g^{\dagger}(\vec{R})\vec{\epsilon}_L\cdot\vec{\Psi}_f(\vec{R}) + \text{H.c.}\Big]. \tag{65}$$

This Hamiltonian describes a sum of independent bosons at each spatial position. Since the motion in the trap potentials is frozen within the duration of the pulse, the Hamiltonian does not contain any information about the trap potentials. In the position representation the Heisenberg equations for the atomic fields are local, and do not couple atomic operators at different locations. But, of course, this does not mean that the trap potential does not play any role. On the contrary, it determines the initial conditions for the Heisenberg equations for the atomic fields. These conditions correspond to BED for the atoms that are in the ground electronic state in the trap. This initial BED is thus related directly to the expansion (62) and (63) and can be most conveniently expressed as a vacuum state for the operators $\vec{\Psi}_f(\vec{R})$ and in terms of the operators $g_{\vec{n}}^{\dagger}$, $g_{\vec{n}}$.

The reason why we could neglect the dependence on $\omega_{\vec{n}}^g$ and $\omega_{\vec{m}}^e$ in (65) is that the relevant motion in the trap (ω_t) is much slower than the coherent driving process (γ_L). Motion is not effected by the trap potentials within the duration of the laser pulse. It is thus tempting to check whether the similar situation holds for atom-atom interactions.

Let us begin the discussion with short range atom-atom interactions responsible for atomic collision processes, and postpone the discussion of long range dipole-dipole forces for a moment. In order to include short range atom-atom interactions in the Hamiltonian Eq. (65), one has to add three terms [12] describing ground-ground, ground-excited, and excited-excited interactions. Within the shape-independent approximation these terms all have the following form [12]:

$$\mathcal{H}_{gg} = \frac{b_{gg}}{2}\int d\vec{R}\;\Psi_g^{\dagger}(\vec{R})\Psi_g^{\dagger}(\vec{R})\Psi_g(\vec{R})\Psi_g(\vec{R}), \tag{66}$$

$$\mathcal{H}_{ge} = b_{ge}\int d\vec{R}\;\Psi_g^{\dagger}(\vec{R})\vec{\Psi}_f^{\dagger}(\vec{R})\cdot\vec{\Psi}_f(\vec{R})\Psi_g(\vec{R}), \tag{67}$$

$$\mathcal{H}_{ee} = \frac{b_{ee}}{2}\int d\vec{R}\;\vec{\Psi}_f^{\dagger}(\vec{R})\cdot\big[\vec{\Psi}_f^{\dagger}(\vec{R})\cdot\vec{\Psi}_f(\vec{R})\big]\cdot\vec{\Psi}_f(\vec{R}), \tag{68}$$

where

$$b_{gg,ge,ee} = 4\pi a_{gg,ge,ee}/M, \tag{69}$$

with a_{gg}, a_{ge}, and a_{ee} denoting the scattering length for the ground-ground, ground-excited, and excited-excited interactions, respectively. Note that the addition of atom-atom interactions to the Hamiltonian (65) does not affect its locality–it remains still a sum of independent contributions at different locations due to the shape-independent approximation [12,23].

Obviously, atom-atom interactions introduce collective energy level shifts and deform atomic wave functions. We can estimate those shifts from perturbation theory to be, at worst, of the order of the quantity $b_{gg,ge,ee}$ times the atomic density. Taking the density to be N/a^3, the scattering lengths $a_{gg,ge,ee}$ to be of the order of few nanometers, and $N = 10^8$, these shifts are at most of the order of 1 MHz. This estimate is, in fact, exaggerated since, in reality, due to atom-atom repulsion, the density of the system will be much smaller (for positive scattering lengths as required for the BEC). The latter statement can be shown to be true in the framework of self-consistent Bogoliubov-Hartree theory (see, for instance, Ref. [12] and references therein). As we see, the shifts are large in comparison with ω_t, and definitely play a crucial role in the long time behavior of the system. They do, in fact, determine equilibrium properties of the system. On the other hand, they can be safely neglected within the duration of the short laser pulse, since they are much smaller than γ_L.

The only interactions which are not yet accounted for are the collective dipole-dipole interactions due to the exchange of transverse photons. They were eliminated from the theory, due to the linearization procedure discussed in Sec. II. But similar arguments as presented above allow us to neglect the dipole-dipole shifts within the duration of the pulse. The magnitude of these shifts can be estimated to be $Nd^2/a^3 \simeq N\gamma/(k_La)^3$, where d is the electronic transition dipole moment. For $N = 10^8$ the dipole-dipole shifts are of the order of GHz. Neglecting them is therefore already quite reasonable for 100 ps pulses, and becomes more appropriate for shorter pulses.

All these estimates show that the Hamiltonian (65) is *generally valid within the duration of the laser pulse* for class A, B, and C models provided that the collective spontaneous emission rate stays small compared to γ_L. The differences between various classes of models come from the fact that each of them may impose different initial conditions for the Heisenberg equations of motion of the atomic operators.

It is also interesting to observe that in order to calculate the spectra it is sufficient to know the equilibrium density of the system, the density-density correlation function, and their respective Fourier transforms. Elementary calculations, analogous to those discussed in preceding sections, yield

$$C(\vec{k},\mu) = \frac{1}{\gamma_L^2}|\varrho(k)|^2|\vec{\epsilon}_L\cdot\vec{\epsilon}_{\vec{k}\mu}|^2 \int d\vec{R}\int d\vec{R}'\left\{\left\langle\left[\Psi_g^\dagger(\vec{R})\Psi_g(\vec{R})e^{i(\vec{k}-\vec{k}_L)\cdot\vec{R}}\right]\left[\Psi_g^\dagger(\vec{R}')\Psi_g(\vec{R}')e^{-i(\vec{k}-\vec{k}_L)\cdot\vec{R}'}\right]\right\rangle W_{\rm coh}(\varpi)\right.$$
$$\left.+\left\langle\left[\Psi_g^\dagger(\vec{R})\vec{\epsilon}_L\cdot\vec{\Psi}_f(\vec{R})e^{i(\vec{k}-\vec{k}_L)\cdot\vec{R}}\right]\left[\vec{\epsilon}_L\cdot\vec{\Psi}_f^\dagger(\vec{R}')\Psi_g(\vec{R}')e^{-i(\vec{k}-\vec{k}_L)\cdot\vec{R}'}\right]\right\rangle W_{\rm in}(\varpi)\right\}. \quad (70)$$

In particular, the coherent spectrum becomes

$$C_{\rm coh}(\vec{k},\mu) = S_{\rm coh}(\varpi)\left|\int d\vec{R}\left\langle\Psi_g^\dagger(\vec{R})\Psi_g(\vec{R})e^{i(\vec{k}-\vec{k}_L)\cdot\vec{R}}\right\rangle\right|^2. \quad (71)$$

As we see, the evaluation of the coherent spectrum requires only the knowledge of the mean atomic density at equilibrium. The above result can be compared to expression (38) for the coherent spectrum obtained for the case of noninteracting atoms. We see that in place of the scattering amplitude defined in Eq. (48), we now have a *form factor* which is the Fourier transform of the mean atomic density distribution. At high temperatures, one can use the Boltzmann distribution with the appropriate size for the spatial density profile. The results for class A and C models do not differ much in this situation. In both cases, the incoherent part of the spectrum does depend on the density-density correlations via $\langle\Psi_g^\dagger(\vec{R})\Psi_g(\vec{R})\Psi_g^\dagger(\vec{R}')\Psi_g(\vec{R}')\rangle$, and accounts for the quantum statistical effects analogous to those considered in the study of the refraction index of a degenerate Bose gas by Morice, Castin, and Dalibard [28]. For low temperatures, below the condensation point, one can construct the mean density for the interacting system using the self-consistent Bogoliubov-Hartree approximation. Here we shall consider only the case $T \simeq 0$, and use the approximate solution of the self-consistent equations [29]

$$\rho^{\rm BEC}(\vec{R}) = \langle\Psi_g^\dagger(\vec{R})\Psi_g(\vec{R})\rangle_{\rm BEC} \simeq \frac{15N_0}{8\pi R_0^5}(R_0^2 - R^2) \quad (72)$$

for $R \le R_0$ and zero otherwise. The size of the condensate in this approximation is given by

$$R_0 = a(60N_0a_{gg}/a)^{1/5}, \quad (73)$$

where a_{gg} refers to ground-ground scattering length.

The coherent spectrum in this approximation becomes

$$C_{\rm coh}^{\rm BEC}(\vec{k},\mu) = S_{\rm coh}(\varpi)\frac{225N_0^2}{\xi^6} \times\left|\sin(\xi)+3\frac{\cos(\xi)}{\xi}-3\frac{\sin(\xi)}{\xi^2}\right|^2, \quad (74)$$

where $\xi = |\vec{k}-\vec{k}_L|R_0$. The above result should be compared to Eq. (45) for the case of noninteracting atoms. As we see, the scattering occurs mainly in the forward direction and is limited in divergence by the size of the condensate R_0. Contrary to the previously discussed case of a noninteracting system, it does not have a Gaussian shape. It decays as $1/\xi^6$, and contains characteristic oscillations in the wings, due to the singularity of the derivative of the density (72) at $R = R_0$. Comparison of the angular distributions obtained for class A and C models is shown in Fig. 7.

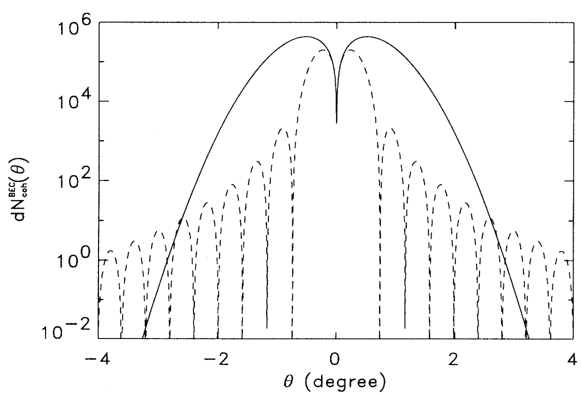

FIG. 7. The angular distribution of coherently scattered photons from the condensate for the class A [solid line calculated from Eq. (38)] and the class C model [dashed line calculated from Eq. (71)] for $N_0 = 10^6$. We have assumed a scattering $a_{gg} = 10^{-4}a = 1$ nm and $\tau_L = 100$ (ps).

VII. CONCLUSIONS

In this work we have investigated theoretically the problem of scattering of intense short laser pulses off a system of cooled atoms. We have presented a detailed theory of such processes, and have examined carefully the regimes of its validity. We have demonstrated that by scattering pulses of area $2\pi K$ one may detect the onset of the Bose-Einstein condensation. In the regime of validity of our theory, $2\pi K$ pulses leave the system of trapped atoms practically unperturbed. Above T_c both coherent and incoherent scattering is very weak and occurs in a very narrow cone in the forward direction due to phase matching effects. As T becomes smaller than T_c, angular distributions of scattered photons as well as their numbers change dramatically. The number of scattered photons increases, while the angular divergence for the coherently scattered photons becomes determined by the condensate size. Scattered radiation is typically super-Poissonian, but might also exhibit squeezing in a narrow range of frequencies at the exact resonance. Most of the theory presented in the paper concerns class A models which neglect atom-atom collisions. We have, however, generalized the theory to include all relevant atom-atom interactions. Using the position representation we have related the spectra to the mean density and the density-density correlation function in the system. For interacting systems, angular distributions of the scattered photons differ from those corresponding to noninteracting systems. Scattering of short laser pulses on a system of trapped atoms thus provides an interesting way to detect the actual state of the system, i.e., its temperature, degree of condensation, etc. It also provides useful information for characterizing the effects of atomic collisions.

We have conducted similar calculations for a system of trapped fermionic atoms. Since the validity of the approximations used in the fermionic case are quite different from the bosonic case, we will present those results and comparative studies between the bosonic and fermionic atoms elsewhere [22].

ACKNOWLEDGMENTS

We acknowledge very fruitful discussions with K. Burnett, I. Cirac, E. Cornell, E. Heller, V. Kharchenko, G. Shlyapnikov, and P. Zoller. L. Y. would like to thank Dr. F. Robicheaux for suggesting a numerical technique for summing the series in Eq. (38). The work of L.Y. and M.L. is supported by the National Science Foundation (NSF) through a grant for the Institute for Theoretical Atomic and Molecular Physics at Harvard University and Smithsonian Astrophysical Observatory. M.L. is also supported by the NSF and Polish Academy of Sciences Grant No. INT-9023548. J.C. is supported by NSF Grant No. PHY90-12244 through the University of Colorado.

APPENDIX A: HARMONIC OSCILLATOR NOTATION

In this appendix we introduce some basic notation for the center of mass motion of atoms in the trap. The trap potential is assumed to be that of an isotropic three-dimensional harmonic potential

$$V_t(\vec{R}) = \tfrac{1}{2}M\omega_t^2 R^2 = \frac{1}{2}M\omega_t^2(x^2+y^2+z^2). \tag{A1}$$

The Hamiltonian $\mathcal{H}_h$ describing the motion in the potential (A1) can thus be represented

$$\mathcal{H}_h = \mathcal{H}_{hx} + \mathcal{H}_{hy} + \mathcal{H}_{hz}, \tag{A2}$$

where

$$\mathcal{H}_{hx} = \hbar\omega_t b_x^\dagger b_x \tag{A3}$$

is a Hamiltonian of a simple one-dimensional harmonic oscillator, for which b_x ($b_x^\dagger$) are the corresponding annihilation (creation) operators. The eigenstates of $\mathcal{H}_h$ can be constructed as

$$|\vec{n}\rangle = |n_x\rangle \otimes |n_y\rangle \otimes |n_z\rangle, \tag{A4}$$

with $|n_x\rangle$ being the eigenvector of $\mathcal{H}_{hx}$. It is easy to check that the trap size (related to the size of the ground state wave function) is

$$a^2 = \tfrac{1}{3}\langle\vec{0}|x^2+y^2+z^2|\vec{0}\rangle = \frac{1}{2M\omega_t}, \tag{A5}$$

and that the position operator can be written as

$$\vec{R} = a\left(b_x^\dagger + b_x, b_y^\dagger + b_y, b_z^\dagger + b_z\right). \tag{A6}$$

APPENDIX B: COHERENT SPECTRUM

In this appendix we give key steps leading to the formula Eq. (38) for the coherent spectrum. We start with the summation as given in Eq. (21)

$$\mathcal{I}_c(\delta\vec{k}) = \sum_{\vec{n}} N_{\vec{n}}\eta_{\vec{n}\vec{n}}(\delta\vec{k}), \tag{B1}$$

where $\delta\vec{k} = \vec{k} - \vec{k}_L$. Using the identity

$$N_{\vec{n}} = \frac{\mathrm{z}e^{-\beta\omega_{\vec{n}}}}{1-\mathrm{z}e^{-\beta\omega_{\vec{n}}}} = \sum_{l=1}^{\infty}\mathrm{z}^l e^{-l\beta\omega_{\vec{n}}}, \tag{B2}$$

we can represent

$$\mathcal{I}_c(\delta\vec{k}) = \sum_{l=1}^{\infty}\mathrm{z}^l \mathcal{I}_{cx}(l)\mathcal{I}_{cy}(l)\mathcal{I}_{cz}(l). \tag{B3}$$

Here,

$$\mathcal{I}_{cx}(l) = \sum_{n_x} e^{-l\beta\omega_t n_x}\langle n_x|e^{-i\delta\vec{k}_x a(b_x^\dagger+b_x)}|n_x\rangle. \tag{B4}$$

Using the Baker-Haussdorf formula [27], and unity decomposition in terms of coherent states

$$1 = \frac{1}{\pi}\int d^2\wp_x|\wp_x\rangle\langle\wp_x|, \tag{B5}$$

we obtain

$$\mathcal{I}_{cx}(l) = e^{\frac{1}{2}\delta k_x^2 a^2}\frac{1}{\pi}\int d^2\wp_x e^{-i\delta\vec{k}_x a\wp_x}e^{-i\delta\vec{k}_x a\wp_x^*} \times \left\langle \wp_x \left| \sum_{n_x}|n_x\rangle\langle n_x|e^{-l\beta\omega_t b_x^\dagger b_x}\right| \wp_x\right\rangle. \tag{B6}$$

The sum over $\vec{n}$ can be easily performed so that

$$\mathcal{I}_{cx}(l) = e^{\frac{1}{2}\delta k_x^2 a^2} \frac{1}{\pi} \int d^2\wp_x e^{-i\delta \vec{k}_x a \wp_x} e^{-i\delta \vec{k}_x a \wp_x^*} \times \exp\left[(e^{-l\beta\omega_t} - 1)\wp_x^* \wp_x\right]. \quad \text{(B7)}$$

The remaining integration over $\wp_x$ yields

$$\mathcal{I}_{cx}(l) = \frac{1}{1 - e^{-l\beta\omega_t}} \exp\left[-\frac{1}{2}\delta k_x^2 a^2 \coth\left(\frac{l\beta\omega_t}{2}\right)\right]. \quad \text{(B8)}$$

Finally we have

$$\mathcal{I}_c(l) = \sum_{l=1}^{\infty} \mathrm{z}^l \frac{1}{(1 - e^{-l\beta\omega_t})^3} \times \exp\left[-\frac{1}{2}\delta k^2 a^2 \coth\left(\frac{l\beta\omega_t}{2}\right)\right]. \quad \text{(B9)}$$

APPENDIX C: INCOHERENT SPECTRUM—THE FLUCTUATION PART

In this appendix we calculate the part of the incoherent spectrum due to the fluctuations of $N_{\vec{n}}$, i.e., the first term in Eq. (35). Thus we need to perform the summation

$$\mathcal{I}_i(\delta\vec{k}) = \sum_{\vec{n}} \delta N_{\vec{n}}^2 \left|\eta_{\vec{n}\vec{n}}(\delta\vec{k})\right|^2 = \sum_{l=1}^{\infty} l\mathrm{z}^l e^{-l\beta\omega_{\vec{n}}^g} \mathcal{I}_{ix}\mathcal{I}_{iy}\mathcal{I}_{iz}, \quad \text{(C1)}$$

where we have defined

$$\mathcal{I}_{ix}(\delta\vec{k}_x) = \sum_{n_x=0}^{\infty} e^{-l\beta\omega_t n_x} \left|\eta_{n_x n_x}(\delta\vec{k}_x)\right|^2 \quad \text{(C2)}$$

and used the identity (which applies to noninteracting bosons—see main text for discussion regarding $\delta N_0^2 = N_0$ being more appropriate when ground state interactions exist).

$$\delta N_{\vec{n}}^2 = N_{\vec{n}}(N_{\vec{n}} + 1) = \sum_{l=1}^{\infty} l\mathrm{z}^l e^{-l\beta\omega_{\vec{n}}^g}. \quad \text{(C3)}$$

It is well known that

$$\eta_{n_x n_x}(\delta\vec{k}_x) = \langle n_x | e^{-i\delta\vec{k}_x a(b_x^\dagger + b_x)} | n_x \rangle = L_{n_x}(\delta k_x^2 a^2) e^{-\frac{1}{2}\delta k_x^2 a^2}, \quad \text{(C4)}$$

where $L_{n_x}(\delta k_x^2 a^2)$ are the Laguerre polynomials of order n_x (see, for instance, [27]) which has the following integral representation [30]:

$$L_{n_x}(\delta k_x^2 a^2) = \frac{1}{2\pi i} \oint \left(1 - \frac{\delta k_x^2 a^2}{\tau}\right)^{n_x} \frac{e^\tau}{\tau} d\tau. \quad \text{(C5)}$$

Therefore, we obtain

$$\begin{aligned}\mathcal{I}_{ix}(\delta\vec{k}_x) &= \frac{1}{2\pi i} \oint \frac{e^\tau}{\tau} d\tau \sum_{n_x=0}^{\infty} e^{-l\beta\omega_t n_x} \langle n_x | e^{-i\delta\vec{k}_x a(b_x^\dagger + b_x)} | n_x \rangle e^{-\frac{1}{2}\delta k_x^2 a^2} e^{n_x \ln(1 - \frac{\delta k_x^2 a^2}{\tau})} \\ &= \frac{1}{2\pi i} \oint \frac{e^\tau}{\tau} d\tau e^{-\frac{1}{2}\delta k_x^2 a^2} \frac{1}{1 - e^{-\tilde{\beta}_l(\tau)}} \exp\left[-\frac{1}{2}\delta k_x^2 a^2 \coth\left(\frac{\tilde{\beta}_l(\tau)}{2}\right)\right]. \end{aligned} \quad \text{(C6)}$$

In the above expression, we have used the same method as described in Appendix B to perform the summation over $\vec{n}$. We have also defined

$$\tilde{\beta}_l(\tau) = l\beta\omega_t - \ln\left(1 - \frac{\delta k_x^2 a^2}{\tau}\right). \quad \text{(C7)}$$

It is easy to check that the following identity holds:

$$\coth\left(\frac{\tilde{\beta}_l(\tau)}{2}\right) = \coth\left(\frac{l\beta\omega_t}{2}\right) - \frac{2}{1 - e^{-l\beta\omega_t}} \frac{\tau_0}{\tau + \tau_0}, \quad \text{(C8)}$$

where

$$\tau_0 = \frac{\delta k_x^2 a^2 e^{-l\beta\omega_t}}{1 - e^{-l\beta\omega_t}}. \quad \text{(C9)}$$

We change the integration variable in Eq. (C6) to

$$\tau' = \tau + \tau_0, \quad \text{(C10)}$$

and arrive at the final expression

$$\mathcal{I}_{ix}(l) = \frac{1}{1 - e^{-l\beta\omega_t}} e^{-\frac{1}{2}\delta k_x^2 a^2} e^{-\tau_0} I_0(2\tau_0 e^{\frac{l\beta\omega_t}{2}}) \times \exp\left[-\frac{1}{2}\delta k_x^2 a^2 \coth\left(\frac{l\beta\omega_t}{2}\right)\right], \quad \text{(C11)}$$

where $I_0(x)$ denotes the zeroth order modified Bessel function [30].

As we shall see below, the part of the incoherent spectrum calculated in this appendix cancels out from the final expression for the total incoherent spectrum. Nevertheless, we have decided to include this appendix, since the method developed above can be useful in other cases (one-dimensional traps, anisotropic traps, weakly interacting atoms in traps).

APPENDIX D: INCOHERENT SPECTRUM

To complete the calculation of the first two terms in Eq. (35) for the incoherent spectrum, we observe that

$$\begin{aligned}\mathcal{I}_i(\delta\vec{k}) &= \sum_{\vec{n}}\sum_{\vec{m}\neq\vec{n}} N_{\vec{n}}(N_{\vec{m}}+1)\left|\eta_{\vec{n}\vec{m}}(\delta\vec{k})\right|^2 \\ &= \sum_{\vec{n},\vec{m}} N_{\vec{n}}(N_{\vec{m}}+1)\left|\eta_{\vec{n}\vec{m}}(\delta\vec{k})\right|^2 \\ &\quad -\sum_{\vec{n}} \delta N_{\vec{n}}^2\left|\eta_{\vec{n}\vec{n}}(\delta\vec{k})\right|^2. \end{aligned} \tag{D1}$$

The above formula shows that the statistical fluctuation part calculated in Appendix C will cancel the second term in Eq. (D1). The first term, on the other hand, can be expressed as

$$\mathcal{I}_i^{(1)}(\delta\vec{k}) = N + \sum_{l_1,l_2=1}^{\infty} z^{l_1+l_2}\mathcal{I}_{ix}^{(1)}\mathcal{I}_{iy}^{(1)}\mathcal{I}_{iz}^{(1)}, \tag{D2}$$

where

$$\mathcal{I}_{ix}^{(1)}(\delta\vec{k}_x) = \sum_{n_x,n_x'=0}^{\infty} e^{-(l_1 n_x+l_2 n_x')\beta\omega_t}\left|\eta_{n_x n_x'}(\delta\vec{k}_x)\right|^2. \tag{D3}$$

In order to evaluate the above expression, we use a technique similar to that discussed in Appendix B: we employ the Baker-Haussdorf formula [27] and introduce the decomposition of unity in coherent states. The summation over n_x and n_x' can then be easily performed, and we obtain

$$\mathcal{I}_i^{(1)}(\delta\vec{k}) = \frac{1}{\pi}\int d^2\wp_x e^{-i\delta k_x a(\wp_x^*+\wp_x)}\langle\wp_x|e^{-l_2\beta\omega_t b_x^\dagger b_x}e^{i\delta k_x a b_x^\dagger}e^{i\delta k_x a b_x}e^{-l_1\beta\omega_t b_x^\dagger b_x}|\wp_x\rangle. \tag{D4}$$

The above integral turns out to be Gaussian and, after elementary calculations, we obtain the final formula:

$$\mathcal{I}_{ix}^{(1)}(\delta\vec{k}_x) = \frac{1}{1-e^{-(l_2+l_1)\beta\omega_t}}\exp\left[-\delta k_x^2 a^2\frac{(1-e^{-l_1\beta\omega_t})(1-e^{-l_2\beta\omega_t})}{1-e^{-(l_2+l_1)\beta\omega_t}}\right], \tag{D5}$$

which was used in Section IV.

[1] (a) J. M. Doyle, J. C. Sandberg, I. A. Yu, C. L. Cesar, D. Kleppner, and T. J. Greytak, Phys. Rev. Lett. **67**, 603 (1991); (b) C. R. Monroe, E. A. Cornell, C. A. Sackett, C. J. Myatt, and C. E. Wieman, *ibid.* **70**, 414 (1993); (c) W. Ketterle, K. B. Davis, M. A. Joffe, A. Martin, and D. E. Pritchard, *ibid.* **70**, 2253 (1993); (d) I. D. Setija, H. G. C. Werij, O. J. Luiten, M. W. Reynolds, T. W. Hijmans, and J. T. M. Walraven, *ibid.* **70**, 2257 (1993); (e) R. J. C. Spreeuw, C. Gerz, L. S. Goldner, W. D. Phillips, S. L. Rolston, C. I. Westbrook, M. W. Reynolds, and I. F. Silvera, *ibid.* **72**, 3162 (1994).

[2] J. Opt. Soc. Am. B **6** (11) (1989); S. L. Gilbert and C. E. Wieman, Opt. Photonics News **4**, 8 (1993).

[3] *Proceedings of the Fourteenth International Conference on Atomic Physics, Boulder, Colorado, 1994*, edited by D. J. Wineland, C. E. Wieman, and S. J. Smith (AIP, New York, 1995).

[4] (a) W. Petrich, M. H. Anderson, J. R. Ensher, and E. A. Cornell, in *Abstracts of Contributed Papers of the Fourteenth International Conference on Atomic Physics* (International Conference on Atomic Physics, Boulder, Colorado, 1994); (b) K. B. Davis, M. O. Mewes, M. A. Joffe, and W. Ketterle, *ibid.*; (c) S. Chu, private communication.

[5] (a) H. F. Hess, G. P. Kochanski, J. M. Doyle, N. Masuhara, D. Kleppner, and T. J. Greytak, Phys. Rev. Lett. **59**, 672 (1987); (b) R. van Roijen, J. J. Berkhout, S. Jaakkola, and J. T. M. Walraven, *ibid.* **61**, 931 (1988); (c) N. Masuhara, J. M. Doyle, J. C. Sandberg, D. Kleppner, T. J. Greytak, H. F. Hess, and G. P. Kochansky, *ibid.* **61**, 935 (1988); (d) C. Monroe, W. Swann, H. Robinson, and C. Wieman, *ibid.* **65**, 1571 (1990).

[6] I. F. Silvera and J. T. M. Walraven, in *Progress in Low Temperature Physics*, edited by D. F. Brewer (Elsevier, The Netherlands, 1986); J. T. M. Walraven, in *Proceedings of the Fourteenth International Conference on Atomic Physics* (Ref. [3]).

[7] B. Svistunov and G. Shlyapnikov, Zh. Eksp. Teor. Fiz. **97**, 821 (1990) [Sov. Phys. JETP **70**, 460 (1990)]; *ibid.* **98**, 129 (1990) [**71**, 71 (1990)].

[8] H. D. Politzer, Phys. Rev. A **43**, 6444 (1991).

[9] J. Javanainen, Phys. Rev. Lett. **72**, 2375 (1994).

[10] (a) M. Lewenstein, L. You, and J. Cooper, in Proceedings of the International Conference on Quantum Optics III, Szczyrk, Poland, 1993, edited by M. Kolwas and J. Mostowski [Acta Phys. Polon. A **86**, 173 (1994)]; (b) L. You, M. Lewenstein, and J. Cooper, Phys. Rev. A **50**, R3565 (1994).

[11] M. Lewenstein and L. You, Phys. Rev. Lett. **71**, 1339 (1993).

[12] M. Lewenstein, L. You, J. Cooper, and K. Burnett, Phys. Rev. A **50**, 2207 (1994).

[13] See Refs. [1(b)], [4(a)], [5(d)], [10], [11], [12].

[14] With the exclusion of the so called *contact term*. E. A. Power and S. Zienau, Philos. Trans. R. Soc. **251**, 427 (1959); as shown in Ref. [10(b)], this term does not seem to play a crucial role.

[15] C. Cohen-Tannoudji, J. Dupont-Roc, and G. Grynberg, *Atoms and Photons, Introduction to Quantum Electrodynamics* (Wiley, New York, 1989).

[16] Recent calculations indicated that the effective collective spontaneous emission rate is of the order of tens of GHz for the parameters considered here; see Refs. [9] and [10].

[17] K. Rzążewski and M. Florjańczyk, J. Phys. B **17**, L509

(1984); E. J. Robinson and P. R. Berman, J. Phys. B **17**, L847 (1984).

[18] K. Rzążewski, Phys. Rev. A **28**, 2565 (1983); M. Lewenstein, J. Zakrzewski, and K. Rzążewski, J. Opt. Soc. Am. B **3**, 22 (1986); M. Florjańczyk, K. Rzążewski, and J. Zakrzewski, Phys. Rev. A **31**, 1558 (1985); Zakrzewski, J. Phys. B **19**, 2247 (1986).

[19] S. R. de Groot, G. J. Hooyman, and C. A. ten Seldam, Proc. R. Soc. London, Ser. A **203**, 266 (1950).

[20] V. Bagnato, D. E. Pritchard, and D. Kleppner, Phys. Rev. A **35**, 4354 (1987).

[21] In Ref. [11], a minor typographical error occurred in the same formulas. It was shown there as $\pi^2 x^2$ instead of the correct formula πx^2.

[22] L. You and M. Lewenstein (unpublished).

[23] See, for instance, A. L. Fetter and J. D. Walecka, *Quantum Theory of Many-Particle Systems* (McGraw-Hill, New York, 1971); A. Griffin, *Excitations in a Bose-Condensed Liquid* (Cambridge University Press, Cambridge, 1993).

[24] It is generally believed, that in the presence of even infinitesimally small interactions the condensation will occur into a coherent state [23]. We adopt here this assumption even though, rigorously speaking, class A models neglect atom-atom interactions and lead to $\delta N_0^2 = N_0(N_0+1)$.

[25] H. P. Yuen and V. W. S. Chan, Opt. Lett. **8**, 177 (1983).

[26] M. Belsley, D. T. Smithey, M. G. Raymer, and J. Mostowski, Phys. Rev. A **46**, 414 (1992).

[27] C. W. Gardiner, *Quantum Noise* (Springer Verlag, Berlin, 1992).

[28] O. Morice, Y. Castin, and J. Dalibard, Phys. Rev. A **51**, 3896 (1995).

[29] V. V. Goldman, I. F. Silvera, and A. J. Leggett, Phys. Rev. B **24**, 2870 (1981).

[30] M. Abramowitz and I. Stegun, *Handbook of Mathematical Functions* (Dover, New York, 1974).